CNRS
Centre National
de la Recherche Scientifique

NIKHEF
Nationaal Instituut
voor Subatomaire Fysica

INFN
Istituto Nazionale
di Fisica Nucleare

Motivations for replacing the current test masses with new ones

VIR-0330A-24

Alessio Rocchi and Fiodor Sorrentino

Issue:
Date: April 7, 2024

VIRGO * A joint CNRS-INFN-NIKHEF Project
Via E. Amaldi, 56021 S. Stefano a Macerata - Cascina (Pisa), Italy
Telephone (+39) 050 752 511 * Email info@ego-gw.it

Contents

1 Scope of this document

Scope of this document is to summarize in a single source the reasons for replacing the current test masses with new ones, with the same polishing requirements, but with better coatings: less point absorbers, higher uniformity and, if possible, lower mechanical losses.

The experiences of LIGO commissioning for O3 and of Virgo in preparation to O4 are reported and provide enough data to support the request.

2 aLIGO experience

Most of the information in this section is taken from [1] and references there in.

Measurements performed at the two LIGO sites using Hartmann wave-front sensors have detected unambiguous evidence of point absorbers on at least 5 of 8 observed test masses [2]. In most cases the point absorbers were demonstrated to be inside of the HR mirror coating [1].

2.1 Power Recycling Gain

One of the first observed effects of the presence of PAs was the decay of the carrier power recycling gain as a function of input laser power. Figure 1 shows the power-recycling gain versus the input laser power over a 4-months period in early 2019 for the two LIGO interferometers, Livingstone (LLO) and Hanford (LHO), with two epochs plotted for LLO. In fact, after an initial commissioning period the Livingston interferometer was realigned to move the laser beam by approximately 30 mm on one of the end test masses [3]. To underline this effect, Livingston data have been labeled as pre- and post-interferometer realignment, red and blue dots, respectively. For Hanford, only optimum alignment is shown (green data). Data in Figure 1 are well explained by modeling the arm cavity losses as

$$\mathcal{L} = \mathcal{L}_0 + b \cdot P^2 \tag{1}$$

i.e. as a power-independent loss $\mathcal{L}$ plus a quadratic term in the circulating optical power P [1]. According to experimental data, PAs contribution to round-trip optical losses in LIGO arm cavities during O3 was of the order of 1 ppm for a circulating power of 100 kW.

Besides the steady state condition discussed above, a rapid drop in the power recycling gain with a time scale of about 200 s is observed at LLO, during a power-up (see blue-dotted line in Figure 2). Using a combination of

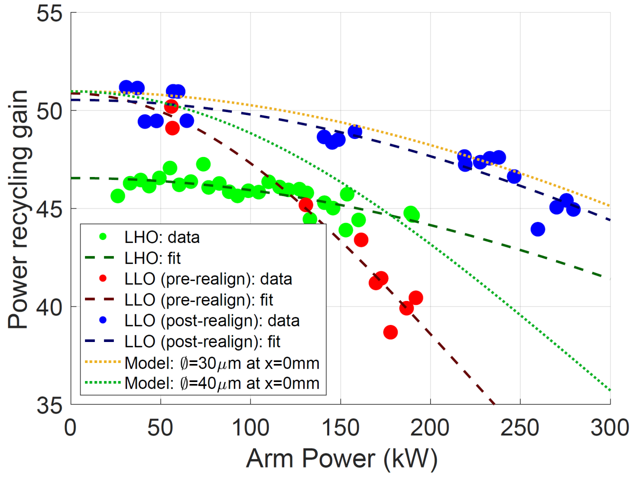

Figure 1: Average LIGO power recycling gain versus arm power for the first 120 days of 2019. Also models predicting the behavior of the PRG are shown with dotted yellow and green curves (assuming 30 μm and 40 μm diameter point absorbers in the center of the test mass, respectively). Reproduced from [1].

finite-element modeling and FFT simulation of the full interferometer, the time evolution of the power recycling gain has been simulated for two different thermal distortions: uniform absorption and a point absorber located approximately 20 mm from the center of the test mass. As the results show, the observed rapid drop in recycling gain is in very good agreement with the point-absorber model.

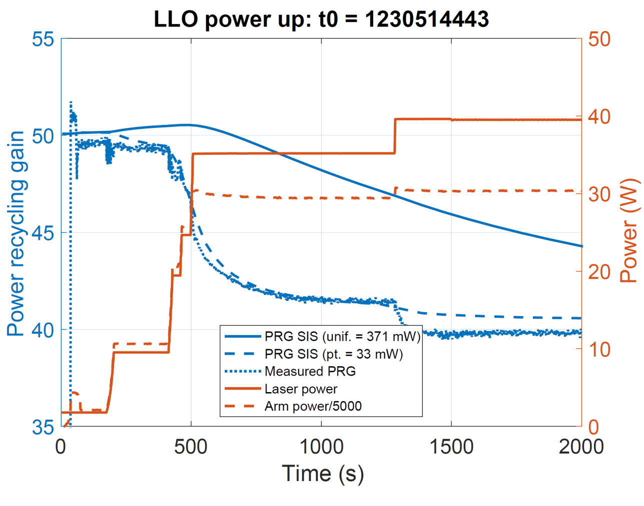

Figure 2: Time evolution of power recycling gain during a power-up at LLO. Laser power and scaled arm power are indicated by the right-hand axis. Power recycling gain is shown on the left-hand axis. Also shown are two models of assuming surface thermo-elastic deformation on one ETM from, uniform absorption and a point absorber, respectively. Reproduced from [1].

2.2 Arm cavities power build-up

During the commissioning phase in preparation of the third observing run (O3), the laser power was increased from 25 W to 40 W. However, this operation did not result in a proportional increase in optical power in the arm cavities, as it can be seen from Figure 3. The loss of power build-up could not be recovered with adjustments to the thermal compensation system actuators. As discussed in Section 2.1, also the amount of power stored in the arm cavities depends on the beam spot position on the test masses. These features indicate nonuniform absorption as the source of the increased optical losses.

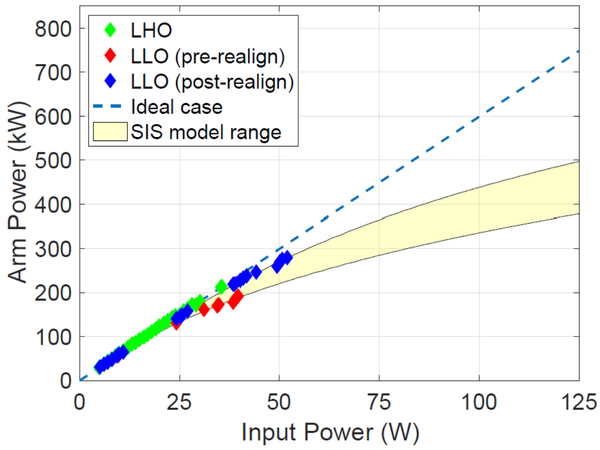

Figure 3: Arm power as a function of the input laser power. The dashed line shows the case of constant optical losses. The data points refer to the measurements done at LIGO, while the yellow range shows predictions from optical simulations assuming both uniform absorption and a variety of point absorbers. Reproduced from [1].

Figure 3 also shows the projected arm power versus input power assuming the optimistic scenario in which only power-dependent losses actually matter (the yellow band). This projection considers the data acquired so far (LHO (green), LLO pre-realignment (red) and post-realignment (blue)) and predicts a significant reduction in the maximum stored power (and, hence, performance) for aLIGO.

2.3 Noise coupling and ITF control

The results of the measurement [1] of the coupling of the input laser relative intensity noise (RIN) to differential arm motion (DARM) in aLIGO have shown that, for frequencies above 500 Hz, the coupling was approximately two orders of magnitude higher than expected from simulations of an ideal interferometer. However, when simulations included optical distortions from point absorbers, a significant increase in high frequency RIN coupling, sufficient to explain the excess coupling observed in the interferometer, was put in evidence.

Moreover, the scattering of power from the fundamental Carrier or Sidebands modes, due to optical aberrations, is responsible for the generation of offsets [1] in the longitudinal locking loops, which, in turn, further increase noise couplings.

Despite the laser intensity contribution to overall noise is not yet a limiting noise source, the coupling, and hence the noise contribution, is expected to increase as arm cavity power increases in future.

Finally, it must be noted that [4], despite LIGO having stable recycling cavities, the alignment of the signal recycling mirror was problematic. In fact, the higher-order modes generated by thermal distortions in the input test masses produced competing stray signals that dramatically affected the design error signal response to signal recycling cavity misalignment. This has forced the LIGO commissioning team to look for different strategy and error signals to control the alignment of the signal recycling mirror.

3 Virgo commissioning experience

The test masses currently in use in Virgo were installed for AdV, i.e. before the O2 science run (circa 2016). However, one of them, namely the NE mirror, was replaced with a spare on June 2023.

3.1 Mechanical losses

The original motivation for NE mirror replacement was to mitigate mechanical losses. All test masses underwent mechanical shocks at the time of the monolithic suspensions failure before O2 commissioning; as a result, several cracks are present at different locations, in particular on some of the glass clamps and/or on the glass ears, and in some cases the contact surface between clamp and ear is rather limited. This is particularly evident on the WI and NE test masses. The quality factor of various bulk modes for the WI mirror and for the original NE mirror is shown in Figure 4; the quality factor of several internal modes decreased with time from 2020 to 2023, in some cases by one order of magnitude.

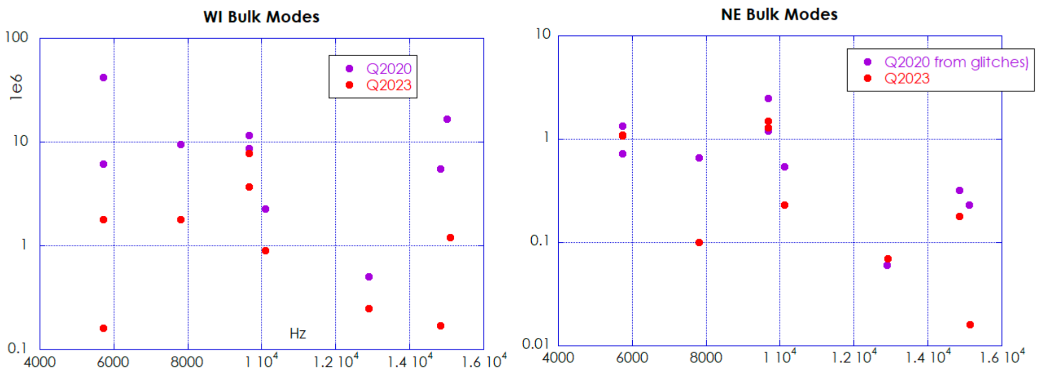

Figure 4: Quality factor of bulk modes for AdV WI and NE test masses as measured in 2020 (purple dots) and in 2023 (red dots).

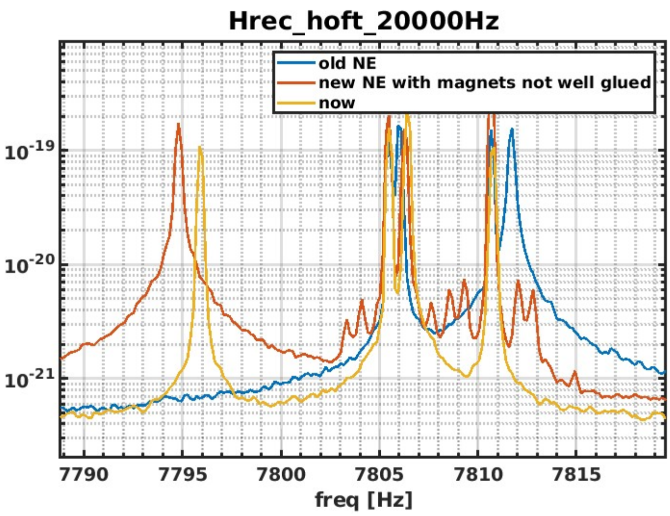

Figure 5: Drum mode of the Virgo test masses before (blue trace) and after (red and yellow traces) replacing the NE mirror with a spare.

Right after the replacement of NE mirror, the Q-factor of the NE drum mode was basically unchanged, however one of the actuation magnet was found to be weakly bound to the new mirror. After improving the magnet adhesion to the test mass, the NE drum mode was largely improved, see Figure 5.

An upper limit to the thermal noise from mechanical dissipation of bulk modes in Virgo arm cavity mirrors was derived by FEM analysis considering the observed quality factors on all test masses after the NE mirror replacement. The result is shown in Figure 6.

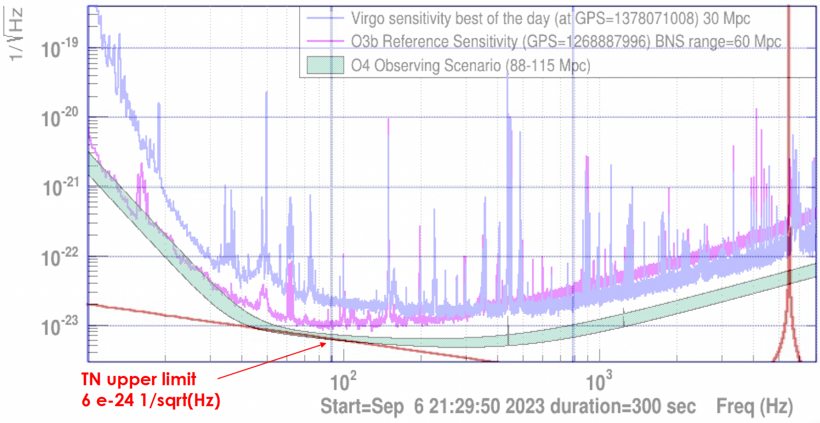

Figure 6: Computed upper limit on strain noise contribution from internal dissipation on Virgo test masses, compared to the typical sensitivity during O3 and to the sensitivity in the middle of O4 commissioning.

3.2 Optical losses

On the other hand, the optical losses after NE mirror replacement were substantially reduced. In particular, this is due to a change in power-dependent losses due absorption and/or scattering, as shown below; however, power-dependent optical losses in Virgo arm cavities are much higher than in LIGO during O3, which were well explained in terms of point absorbers.

3.2.1 Point absorbers

The evidence for point absorbers in Virgo test masses is similar as in LIGO. Figure 7 shows the optical power in Virgo arm cavities after a typical locking sequence with 31 W input laser power: the circulating power reaches a peak value above 150 kW, and then decreases by about 15% with a time constant of the order of one minute.

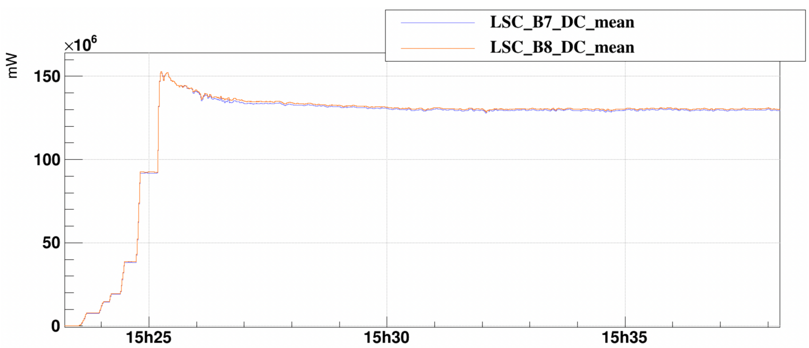

Figure 7: Optical power in Virgo arm cavities (red trace: West arm; blue trace: North arm) during a typical locking sequence with 31 W input laser power.

Point absorbers are also visible on Hartmann images in reflection from input test masses. In at least one case, there is evidence that point absorbers can be due to external contamination instead of being embedded into the coating. Figure 8 shows Hartmann reflection images from the WI mirror at three different times, separated by two vacuum breaks. A point absorber disappeared after the first break, due to a cleaning operation on the mirror's surface. Another point absorber appeared instead after the vacuum break on WI tower to remove a faulty magnet from the test mass on May 2023.

An additional, indirect evidence for non-uniform absorption is the change of arm cavity losses when moving the arm cavity axis across the test masses, as also observed in LIGO. Figure 9 shows the result of such a

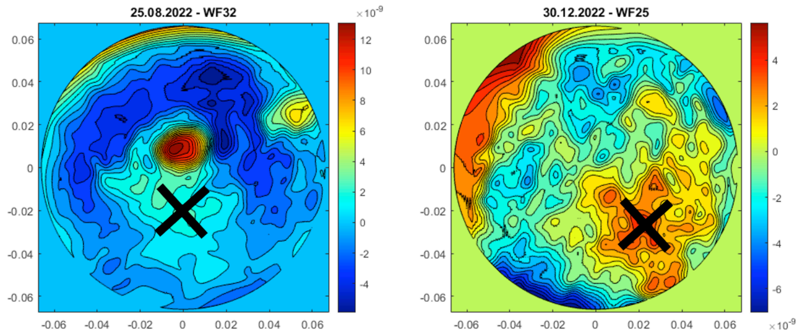

Figure 8: HWS images from the Virgo WI mirror at three different times: left: before monolithic suspension failure (August 2022); center: after mirror cleaning from monolithic suspension failure (December 2022); right: after vacuum break for magnet removal (June 2023). Black crosses show the optical axis center.

measurement during O3 commissioning. The carrier gain could be increased by about 10% when moving the arm cavity axis away from end mirror centers by about 20 mm.

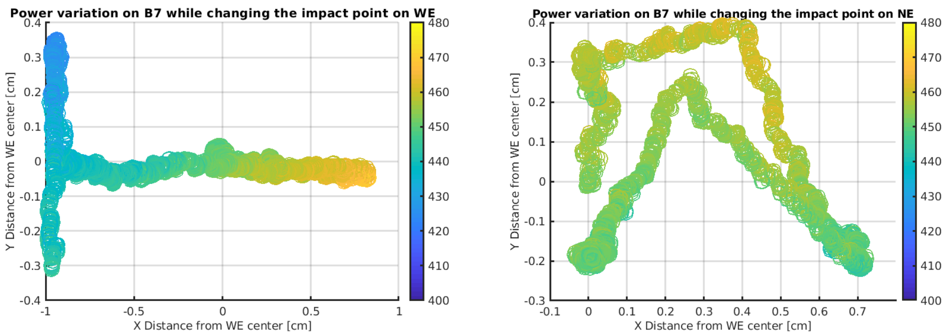

Figure 9: Change in circulating optical power in Virgo arm cavities when moving the position of cavity axis with respect to the center of end test masses; left: cavity axis motion on WE mirror; right: cavity axis motion on NE mirror. From [7]

3.2.2 Power-dependent losses

As the Virgo interferometer was operated with a set of different values of input laser power during O4 commissioning, it is possible to estimate the power-dependent contribution to optical losses in arm cavities. Figure 10 shows the evolution of carrier recycling gain, computed from mean arms circulating power and input laser power over one year, together with the corresponding round-trip losses in arm cavities. Round-trip losses $\mathcal{L}$ are computed from the measured carrier recycling gain G, PR mirror reflectivity R and transmission T, and arm cavity finesse $\mathcal{F}$:

$$G = \frac{T}{\{1 - \sqrt{R}[1 - \mathcal{F}\mathcal{L}/\pi]\}^2} \tag{2}$$

assuming that the contribution of PRC losses to PRC gain is small compared to the contribution from arm cavity losses, which are weighted by the arm cavity finesse.

The main changes in measured arms losses were due to changes in the input power, and to the replacement of NE mirror [5]. Gain changes after vacuum breaks on WI and NE mirrors, e.g. due to the appearance of new PAs, are much smaller than the change due to the replacement of the NE mirror.

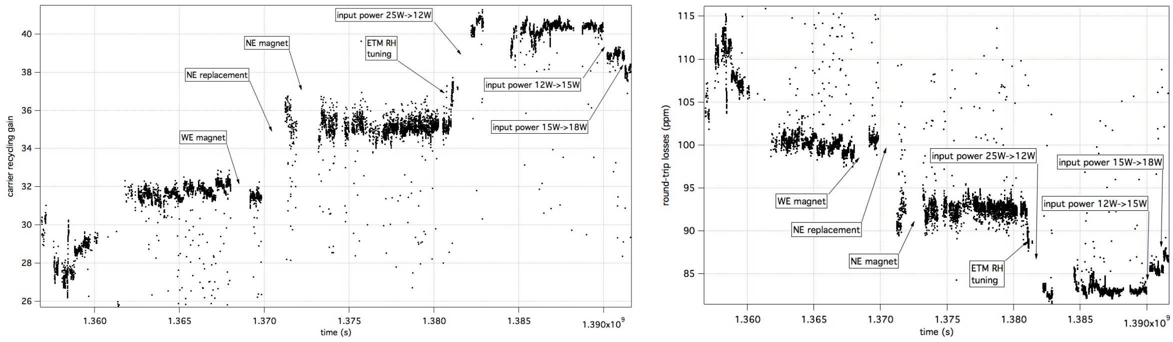

Figure 10: Left: time evolution of the carrier recycling gain over one year starting from January 2023; right: time evolution of the corresponding round-trip losses in arm cavities over the same period.

To extract the power-dependent term in the optical losses $\mathcal{L}$, the carrier recycling gain and the corresponding RTL are plotted versus laser power, as shown in Figure 11. Data before and after NE mirror replacement can be separately fitted with a linear dependence of RTL on optical power. From the linear fit, the power-dependent extra RTL was about 25 ppm for a circulating power of 100 kW with the old NE mirror, and about 25% lower with the new NE mirror. So the power-dependent losses in Virgo arm cavities are more then one order of magnitude higher than in LIGO during O3. The removal and appearance of PAs on WI mirror surface did not substantially modify arm RTL.

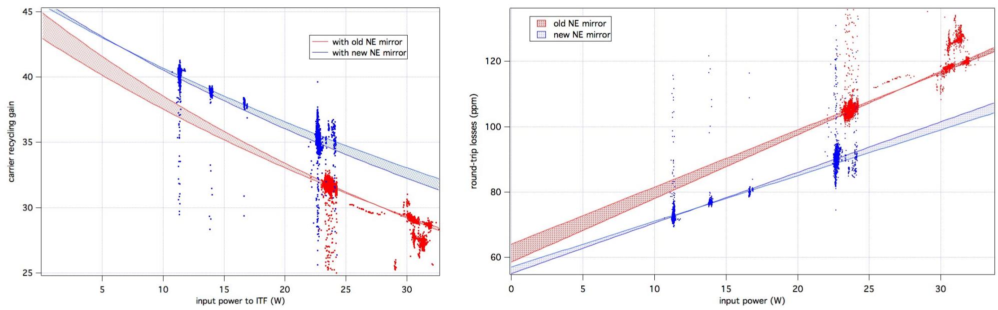

Figure 11: Left: carrier recycling gain versus input laser power in Virgo; right: mean arm round-trip losses versus input laser power in Virgo. Red points: before replacing NE mirror; blue points: after replacing NE mirror. Shaded areas represent linear fit of round trip losses versus input power.

Using the power-dependent loss derived above, it is possible to extrapolate the circulating power in Virgo arm cavities versus input laser power, as shown in Figure 12. The data clearly show that increasing the input power will not result in a proportional increase in optical power in the arms. It also shows that with the original set of O2 mirrors it would have been impossible to achieve the same circulating power levels as in LIGO during O3; with the new NE mirror, this would anyway require an input laser power of the order of 80 W.

Figure 13 shows the appearance of the old NE mirror's surface right before its removal from the vacuum tower [5]. The nature of the visible inhomogeneity producing large light scattering on the mirror's surface is currently unknown, but it might be related to the much larger power-dependent losses as compared with the effect of PAs in O3 LIGO mirrors.

4 Conclusions

The current test masses in Virgo show both excess mechanical losses and very large power-dependent optical losses.

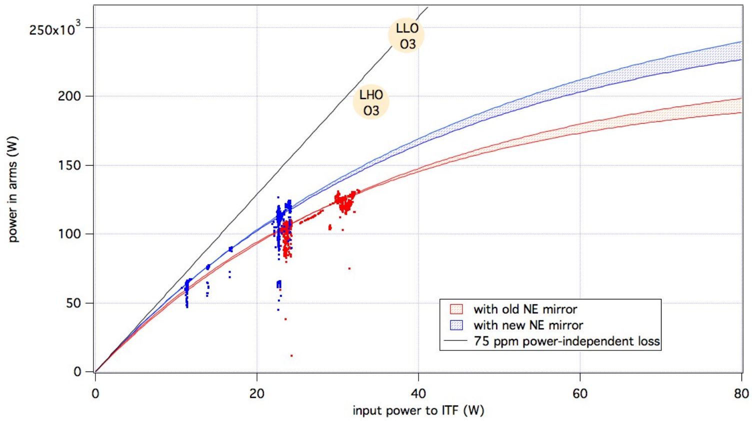

Figure 12: Arms circulating power versus input laser power. Red points: before replacing NE mirror; blue points: after replacing NE mirror. Shaded area are extrapolation from fitted linear power-dependent loss factors. Circles indicate typical values of input power and circulating power for the two LIGO detectors during O3.

Figure 13: Surface of the old NE mirror before its removal from the vacuum tank in June 2023

The issues reported in Section 2 led the LIGO Lab management to decide for the replacement of all test masses during the break between O3 and O4. In fact, in the meantime, the source of the majority of the point absorbers has been identified and removed, so that it has been possible to coat the new mirrors with a considerable reduction of the point defects. This action, among others, has allowed the LIGO detectors to double the amount of power stored in the arm cavities, reaching about 430 kW [6].

Given the issues encountered by Virgo during the O4 commissioning phase with the present mirrors (see Section 3), considering the progresses made by the LIGO detectors after replacing the test masses, it is mandatory also for Virgo to replace the main mirrors in order to achieve the planned [8, 9] amount of optical power circulating in the 3 km long cavities and the expected sensitivity goals.

The currently available mirror spares in Virgo would likely give lower mechanical losses and, as suggested by the effect of replacing the NE mirror, a lower level of power-dependent losses. However, the production of a new set of test masses is necessary for the following reasons:

1. the current spares were produced before a method to avoid point absorbers in the coating was developed at LMA; as a consequence, the best performance in terms of power-dependent optical losses would likely be similar to LIGO in O3;
2. the spare input test masses are poorly matched in terns of HR coating reflectivity, which would generate

a finesse asymmetry between arm cavities above the correction range of the Etalon effect;

3. a set of spares would anyway be needed.

References

[1] A. F. Brooks et al., *Point absorbers in Advanced LIGO*, Appl. Opt. **60**, 4047 (2021) 1, 2, 3

[2] G. Billingsley, A.F. Brooks, L. Zhang, *HWS absorption map and Transmission map Comparison O3 Test masses*, LIGO-G1900693, https://dcc.ligo.org/LIGO-G1900693 1

[3] D. Martynov, LLO aLOG 43121, February 2019, https://alog.ligo-la.caltech.edu/aLOG/ 1

[4] A. Buikema et al., *Sensitivity and performance of the Advanced LIGO detectors in the third observing run*, Phys. Rev. D **102**, 062003 (2020) 3

[5] L. Naticchioni et al., Virgo e-log 60459, June 2023, https://logbook.virgo-gw.eu/virgo/?r=60459 6, 7

[6] N. Aritomi, *LHO Commissioning Report*, LIGO-G2301748, https://dcc.ligo.org/LIGO-G2301748 8

[7] A. Allocca and P. Ruggi, Virgo e-log 47029, September 2019, https://logbook.virgo-gw.eu/virgo/?r=47029 6

[8] Virgo Collaboration, *Overview of Advanced Virgo Plus Phase II*, VIR-1179C-19, https://tds.virgo-gw.eu/ql/?c=15013 8

[9] A. Rocchi, *Virgo upgrade plans @ LVK March 2024*, VIR-0251A-24, https://tds.virgo-gw.eu/ql/?c=20311 8